

Control of spin correlations by periodic driving

K. Kudo¹ and T. Boness and T.S. Monteiro²

¹*Division of Advanced Sciences, Ochanomizu Academic Production, Ochanomizu University, 2-1-1 Ohtsuka, Bunkyo-ku, Tokyo 112-8610, Japan*

²*Department of Physics and Astronomy, University College London, Gower Street, London WC1E 6BT, United Kingdom*

(Dated: April 3, 2020)

We investigate transport in an excited 1D Heisenberg ferromagnetic chain, subject to periodic driving from an external magnetic field. The Heisenberg chain exhibits two classes of states: magnon (scattering) states, where the spins propagate separately, and bound-states, where the spins propagate together. We show that the effects of periodic driving, like renormalization of the spin-coupling strength, act selectively on these two types of states. Thus one can control the relative direction and speed of transport of wavepackets of bound and separate spins respectively, even when the initial state is a superposition of both.

PACS numbers: 75.10.Pq, 03.67.Hk, 05.45.Mt

The dynamics of quantum spin transport and in particular spin correlations are of much current interest in the field of quantum information [1]. Quantum correlations are closely related to entanglement between spins, the fundamental resource for quantum information processing. It has been shown that specific correlation dynamics may be designed into an engineered spin chain, by adjusting global physical parameters [2]. Here we show that a type of control can also be achieved, even after the spin-chain has been constructed, and in real time, by applying a global time-periodic external field.

Spin-chains are generally characterised by an exchange coupling strength J . We consider a system with a Heisenberg ferromagnetic Hamiltonian $-JH_{\text{hc}}$ subjected to an additional spatially-linear oscillating field, giving a total time-dependent Hamiltonian:

$$H(t) = -JH_{\text{hc}} - \frac{B}{2} \sin \omega t \sum_{n=1}^N n \sigma_n^Z. \quad (1)$$

One can easily show that for $B, \omega \gg J$, the exchange strength takes an effective, renormalized value:

$$J_{\text{eff}} = J J_0\left(\frac{B}{\omega}\right), \quad (2)$$

where J_0 denotes an ordinary Bessel function. This arises from a generic effect known as Coherent Destruction of Tunneling (CDT) [3] previously investigated in tunneling of a particle in a periodically forced double well. The inter-site coupling can be completely suppressed at values of $\frac{B}{\omega} = 2.4, 5.52..$ corresponding to $J_0(\frac{B}{\omega}) = 0$; and it can even change sign [when $J_0(\frac{B}{\omega}) < 0$]. CDT for cold atoms in optical lattices has been investigated theoretically [4, 5] and recently, the CDT renormalization of J in Eq.(2) was mapped out experimentally using Bose Einstein Condensates [6], since the required linear potential is relatively straightforward to implement using accelerated optical lattices. CDT is a fundamentally quantum effect: it can in principle be realized in a 2-site lattice. It is very closely related to an effect termed Dynamical

Localization [7, 8] (*not* to be confused with the unrelated exponential Dynamical Localization seen in studies of quantum chaos with cold atoms [9]). The relationship between DL and CDT is discussed in detail by [10] but, in brief, we note that DL persists in the limit $N \rightarrow \infty$ and there is no requirement for $\omega \gg J$, i.e. for high-frequency driving.

Our key finding is that multiply excited spin-chains have eigenstates which respond differently the renormalization in Eq.(2). We can thus use this effect to selectively manipulate the transport. In addition, the oscillating linear driving is well-known in studies of ratchets: it very naturally generates directed motion. We can thus split a spin wavepacket and send selected states with different spin correlations, in opposite, or similar directions, at will, with controllable speeds and little dispersion.

The well-known spin-1/2 Heisenberg XXZ ferromagnetic chain of length N , is governed by the Hamiltonian:

$$-JH_{\text{hc}} = -\frac{J}{4} \sum_{n=1}^N [2(\sigma_n^+ \sigma_{n+1}^- + \sigma_n^- \sigma_{n+1}^+) + \Delta \sigma_n^Z \sigma_{n+1}^Z], \quad (3)$$

where $n \in [1 : N]$ indicates the n -th site, and Δ denotes the anisotropy. This Hamiltonian (even including the driving term) conserves the number of spin-flips; a single excitation represents a spin-wave, or magnon, which distributes a single spin-flip throughout the chain. The spin-wave eigenstates of Eq.(3) are

$$|\kappa\rangle = \frac{1}{\sqrt{N}} \sum_{n=1}^N e^{in\kappa} |n\rangle \quad (4)$$

(for a ring; open chains yield a slightly different form [11]) and obey the dispersion relation $E_\kappa - E_0 = -J \cos \kappa$, where E_0 is the ground state. Higher excited-states correspond to multiple spin-waves which interact when they coincide through both an exclusion process (no two spin flips can simultaneously occupy the same site) as well as a mutual interaction induced by the $\sigma_n^Z \sigma_{n+1}^Z$ (Ising) term

— the strength of which is determined by the anisotropy parameter Δ .

We now analyse the two-excitation case. The eigenstates of Eq.(3) may be expressed, via the Bethe ansatz, as spin waves [11, 12]:

$$|\kappa_1, \kappa_2\rangle = A_{\kappa_1, \kappa_2} \sum_{n_1 < n_2 \leq N} a_{n_1, n_2}^{\kappa_1, \kappa_2} |n_1, n_2\rangle. \quad (5)$$

where $A(\kappa_1, \kappa_2)$ is a normalization constant and $|n_1, n_2\rangle$ denotes a state with a spin-flip at sites n_1 and n_2 . Further details are in [11, 13] but the eigenstates divide into two distinct classes: (1) Magnon-like *scattering states*, where the spins move separately, with dispersion relation $E_{\kappa_1, \kappa_2} - E_0 = J(2\Delta - \cos \kappa_1 - \cos \kappa_2)$ which is a straightforward extension of the singly-excited case and (2) *Bound-pair states*, for which the probability amplitudes are at a maximum when the flips are on neighboring sites and they decay exponentially with the separation of the flips. For $\Delta \geq 1$, and as $N \rightarrow \infty$ they obey the dispersion relation, $E_{\kappa_1, \kappa_2} - E_0 = J\Delta - \frac{J}{2\Delta}[1 + \cos(\kappa_1 + \kappa_2)]$. Note that the sum $(\kappa_1 + \kappa_2)$ is always real. In [11] a perturbation expansion in spin coupling strength J is employed to produce an effective Hamiltonian when $\Delta \gg 1$. In this approximation the bound state amplitudes are:

$$a_{n_1, n_2}^{\kappa_1, \kappa_2} = \delta_{n_1, n_2-1} e^{i(\kappa_1 + \kappa_2)n_1} \quad (6)$$

and thus the bound states become confined to the nearest neighbor (NN) subspace, $\{|n, n+1\rangle\}$; their dispersion relation remains unchanged from the above. In “center of mass” coordinates $2\kappa = \kappa_1 + \kappa_2$ the bound states are given by $|\kappa\rangle = A_\kappa \sum_{n=1}^N e^{2n\kappa} |n, n+1\rangle$ and are of analogous form to the single magnon solution Eq.(4): two initially neighboring spin-flips thus transport *together* in a similar way to a lone flip in the single excitation basis $\{|n\rangle\}$ (but their propagation speed is slower: it is scaled by $\frac{J}{2\Delta}$ rather J).

We now turn our attention to CDT in a spin chain. Using units of scaled time $t' = \omega t$, we see that the quantum dynamics generated by Eq.(1) depends, in fact, only on two global parameters $J' = J/\omega$ and $B' = B/\omega$, (for a given Δ). The high-frequency driving condition for CDT thus becomes $J' \ll 1$. We follow the usual procedure for justifying CDT [4]: for $B' \gg J'$, we initially neglect H_{hc} and set $H(t) = -B' \sin t' \sum_{n=1}^N n \sigma_n^Z$.

Then, the Schrödinger equation has the following time-dependent solutions:

$$|n_1, n_2, t\rangle = e^{-iB'(n_1+n_2)\cos t} |n_1, n_2\rangle, \quad (7)$$

to within a constant phase term $e^{iB'\varphi \cos t}$ where $\varphi = \sum_{n=1}^N n = N(N+1)/2$. The stationary states of periodically driven systems (Floquet states) have a Brillouin zone type structure [4] and the above correspond to a family of solutions $|n_1, n_2, m, t\rangle = |n_1, n_2, t\rangle e^{imt}$ which are periodic in time. In multiphoton physics (the study of systems strongly driven by an oscillating electromagnetic field) the band index m is used to label states which

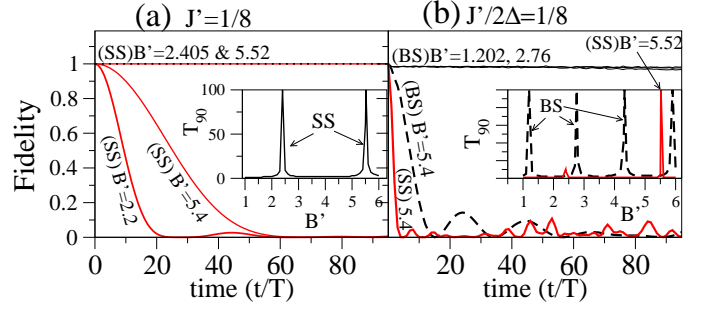


FIG. 1: (color online) CDT demonstrated in an anisotropic chain ($\Delta = 8$) with $N = 20$. An initial state of two adjacent spin flips $|\psi(t=0)\rangle = |n, n+1\rangle$ overlaps only with bound states (BS) while an initial state comprising separated spin-flips $|\psi(t=0)\rangle = |n_1, n_2\rangle = |5, 15\rangle$ overlaps only with magnon-like scattering states (SS). The fidelity $F(t) = |\langle\psi(t=0)|\psi(t)\rangle|^2$ is shown as a function of time. Insets plot T_{90} , the time taken for the fidelity to fall to 0.9, so show the CDT resonances. (a) For small $J'/ = 1/8$, initially separated spin-flips freeze at zeros of $J_0(B')$ so $F(t) = 1$ but delocalize elsewhere. (BS case not shown since $J'/2\Delta \simeq 0$ here). (b) For large $J'/ = 2$ and thus $J'/(2\Delta) = 1/8$ adjacent spin-flips freeze at fields for which $J_0(2B') = 0$, while separated spin-flips freeze at $J_0(B') = 0$ (provided $B' \gg J'$); for this chain, driving at the $B' \simeq 4.3$ resonance freezes adjacent spin-flips; driving at the $B' \simeq 5.52$ resonance freezes initially separated flips, while driving at non-resonant values like $B' = 5.4$ delocalizes both.

differ only by the absorption or emission of m energy quanta (photons) of energy $E_m = m\hbar\omega$. The next step is to treat the spin-exchange as a perturbation, in the extended Hilbert space where time appears as an extra coordinate. The matrix elements of H_{hc} are simply

$$\langle\langle n'_1, n'_2, m', t | JH_{\text{hc}} | n_1, n_2, m, t \rangle\rangle \simeq \delta_{mm'} JJ_0 [B'(n'_1 - n_1) + B'(n'_2 - n_2)] \langle n'_1, n'_2 | H_{\text{hc}} | n_1, n_2 \rangle \quad (8)$$

Where $\langle\langle \cdot | \cdot \rangle\rangle = \frac{1}{T} \int_0^T \langle \cdot | \cdot \rangle$ denotes a scalar product in the extended space [4] and $\langle \cdot | \cdot \rangle$ denotes the scalar product in position coordinates. It is easily seen that in general, the matrix elements $\langle n'_1, n'_2 | H_{\text{hc}} | n_1, n_2 \rangle = [\delta_{n'_1, n_1 \pm 1} \delta_{n'_2, n_2} + \delta_{n'_2, n_2 \pm 1} \delta_{n'_1, n_1}] \langle n'_1, n'_2 | H_{\text{hc}} | n_1, n_2 \rangle$. In other words, they involve hopping of single spins only. Thus, $JJ_0 [B'(n'_1 - n_1) + B'(n'_2 - n_2)] = JJ_0(B')$ as in Eq.(2).

The situation for the bound states in the regime of Eq.(6) is somewhat different. They evolve under an effective Hamiltonian H_{eff} [11] (by means of a second-order process) which results in the two spins hopping together, to the left or to the right. The site to site transport is then determined by matrix elements of the form $\frac{J}{2\Delta} J_0(2B') \langle n, n+1 | H_{\text{eff}} | n+1, n+2 \rangle$ for hopping to the right, or $\frac{J}{2\Delta} J_0(2B') \langle n, n+1 | H_{\text{eff}} | n-1, n \rangle$ for hopping to the left. The important point is the doubling of the argument of the Bessel function. Since the Bessel is an oscillating function, one can, for example, choose a value of the field ratio $B' = B/\omega$ for which $J_{\text{eff}} = JJ_0(2B')$

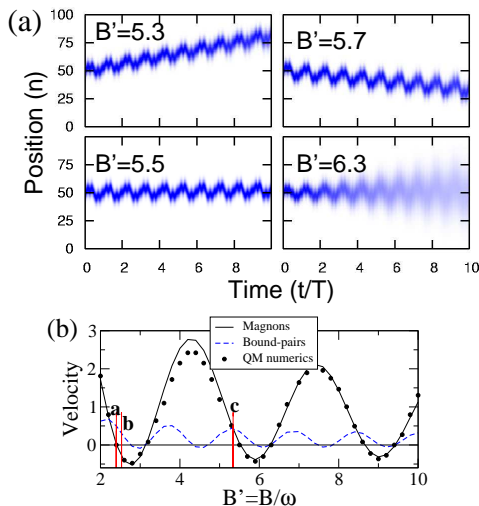


FIG. 2: (color online) (a) Probability distribution for an initial Gaussian spin-wavepacket containing a single excitation, as a function of time, for $J' = 8$. An average velocity is estimated by calculating the centre of mass displacement per period of driving. Two zero-velocity cases are shown: $B' = 5.5$ corresponds to $J_0(B') = 0$ and suppression of spin hopping; while $B' = 6.3$ corresponds to $\sin B' = 0$, so suppression of directed motion, but not of hopping: the spin excitation diffuses along the chain. (b) average velocity of the wavepackets as a function of B' . Numerics were obtained from plots like those in (a). They are well-fitted by the magnon velocity Eq.(9), while the predicted bound state behavior corresponds instead to Eq.(10) shown here for $\Delta = 2$. The vertical lines **a**, **b**, **c** correspond to the multiply excited packets shown in Fig.3.

(for bound-pairs) is positive while $J_{\text{eff}} \simeq JJ_0(B')$ for the magnon-like scattering states is negative. Or one of these can be chosen to correspond to a zero. An arbitrary spin state, for example two spin flips at specific positions, or two Gaussian wavepackets giving two partially localized spin-flips, in general has a projection on both the magnon-like and the bound-pair eigenstates. For large anisotropy, however, one may prepare a good approximation to a pure bound-pair state by simply flipping two adjacent spins of a ferromagnetic chain in its ground state (all spins aligned). Conversely, two well-separated spins will approximate pure magnon-like states.

In Fig.1 we demonstrate CDT for these two cases. Driving with a field $B' = 5.52$ “freezes” two initially well-separated spin-flips at their original sites, since $J_0(B') = 0$. In the absence of driving, or at values of B with $J_0(B') \neq 0$, both spins rapidly diffuse along the chain. On the other hand, if the two-flips are initially *adjacent*, they remain frozen at their positions if $J_0(2B') = 0$ and delocalize otherwise. We can envisage possible applications for correcting errors in the initial state: if some quantum information protocol requires a state with adjacent spins, driving at $2B' = 2.4, 5.52$ etc would ensure rapid dispersion of non-adjacent spins prepared in error, while freezing in place the desired component.

We now turn our attention to Dynamical Localization

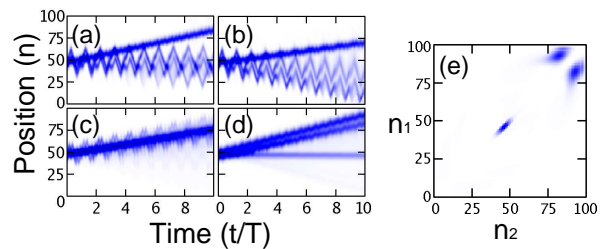


FIG. 3: (color online) Control of bound-pair and magnon spin states for parameters shown in Fig.2(b). (a): $J' = 10$, $\Delta = 2$, $B' = 2.4$. The fast magnon states are stopped, while bound-pairs travel to the end of the spin-chain. (b) $J' = 10$, $\Delta = 2$, $B' = 2.53$. Bound-pair and magnon states move in opposite direction (bound-pairs move towards $N = 100$). (c) $J' = 10$, $\Delta = 2$, $B' = 5.34$. The faster magnon packets are slowed by the field so magnon and bound-pair speeds become equalized and they now travel together. (d) $J' = 2$, $\Delta = 5$, $B' = 4.33$. Bound-pairs remain static, magnons travel. (e) spin-spin correlation at $t/T = 10$ for the spin dynamics of (d). The component with adjacent spins remains stationary, in its initial position at the centre, while the component with separated spins travels to the end of the chain.

(DL). We evolve Eq.(1) for an open chain with $N = 100$ sites. There is no longer a requirement for high-frequency driving so we take, in scaled units $B', J' \gg 1$. To illustrate DL, we prepare a one-spin flip Gaussian wavepacket, at the centre of the chain. Fig.2(a) shows that the spin-packet moves, with little spreading, along the chain, but its direction of travel *reverses* at $B' \simeq 5.5$: for $B' = 5.3$ it moves left, for $B' = 5.7$ it moves right; $B' = 5.5$ it exhibits DL. We highlight a key difference between CDT and DL [7, 10]: while in CDT the spins remain frozen at their original sites, for DL the packet oscillates slightly, but the spins return periodically to their original position. The results for $B' = 6.3$ are at first sight more puzzling: the wavepacket’s centre of mass is static, but the excitation diffuses along the chain. In order to understand these results, one notes that Fig.2(a) represents a combination of DL type renormalisation, as well as a type of directed motion familiar in ratchet physics (arising from broken symmetries in the potential). For the magnon-like excitations, the dispersion relation corresponds to a group velocity $J \sin \kappa_i$. In the presence of driving and in the $N \rightarrow \infty$ limit, one may map the system to an “image” classical Hamiltonian $H(x, p) = -J' \cos p - B' x \sin t'$, by mapping site to continuous position $n \rightarrow x$ and $\kappa \rightarrow p$. The distance travelled per period, for a particle with momentum $p(t=0) = p_0$ is simply:

$$\frac{\langle x \rangle}{2\pi} = J' J_0(B') \sin(p_0 + B') \quad (9)$$

In effect, this is the centre of mass velocity of the wavepacket but shows that it is no longer a question of simply renormalizing J' by $J_0(B')$ because the $\sin(p_0 + B')$ factor can also change sign or suppress transport.

It does provide great advantages in reducing dispersive spreading. An initial gaussian wavepacket, initially localized over a finite number of sites $1/\delta_n$, corresponds to localization in momentum of $\sim \delta_n$, in the image phase-space. Thus the corresponding momentum distribution is $N(p) \sim \exp[-(p_0 - \langle p \rangle)^2/\delta_n^2]$. Spin wavepackets generally correspond to low energy excitations well localized about $\kappa \sim 0$ so we set $\langle p_0 \rangle = 0$. The distribution thus samples velocities $\sim J' J_0(B') \sin(B' \pm \delta_n)$. Hence provided $|B' \pm \delta_n| \lesssim \pi$, all momenta $-\delta_n < p_0 < \delta_n$ correspond to the same direction of motion and there is little dispersion. This results in *directed motion*. In contrast, when $B' \simeq m\pi$, with $m = 1, 2, \dots$ trajectories with $p_0 < 0$ move in opposite direction to $p_0 > 0$ and the wavepacket, though static, spreads diffusively along the chain. In the presence of DL so $J_0(B') = 0$, there is, of course no transport, so no diffusion. In Fig.2(b) we see that a numerical estimate of the velocity (displacement of the quantum wavepacket per period) obtained from a quantum solution of Eq.(1) is in excellent agreement with Eq.(9).

For multiple excitations, we assume that scattering state projection of the wavepackets obey Eq.(9), while the Hilbert space fraction of bound-pair states moves under a different image Hamiltonian $H = \frac{-J'}{2\Delta} \cos 2P - 2B'X \sin t$ where $2P = p_1 + p_2$ and $X = (x_1 + x_2)/2$ indicate centre of mass coordinates. Thus the bound-pair velocity

$$\frac{\langle x_{\text{bs}} \rangle}{2\pi} = \frac{J'}{2\Delta} J_0(2B') \sin(p_0 + 2B') \quad (10)$$

Fig.2(b) (broken line) shows the corresponding velocity. One sees that the bound-pair and magnon velocities may even have opposite signs for the same driving field. This enables us to steer the two components in opposite directions or to stop one and transport the other etc. These different situations are demonstrated in Fig.3, where the initial state is the product of two Gaussian wavepackets at $n_1 = 45$ and $n_2 = 50$. Even for quite modest Δ we see

that the wavepacket quickly splits into two components, whose relative speed and direction may be controlled. This is in contrast to the undriven case: while magnon states diffuse faster than bound-pair components (by a factor of 2Δ) both simply delocalize along the length of the chain. The driving can weakly couple the two subspaces of bound-pair and magnon states (especially for low Δ). However once the wavepackets separate, further interaction is negligible. Fig.3(e) illustrates the spin correlations for Fig.3(d) (for large $\Delta = 5$) where the component with adjacent spins is immobilized and the component with separated spins is transmitted. Obviously there are other variations on this scenario.

One may also consider higher numbers of excitations. Bound-states with exponential localization on sets of $M > 2$ spins are also possible. However, hopping in this case goes as $\sim J/(M\Delta)$, making their propagation speeds rather slow, relative to the scattering states. But one might consider a long chain with several $m > 1$ sets of localized gaussian packets of adjacent spin-flip pairs. In this case, provided the spin-pair packets do not collide, each member of them would approximately move like an independent bound-pair and could be controlled as in Eq.(10).

Finally, we note that these effects are already accessible to experiments with cold atoms in accelerated optical lattices which have energy dispersion relation for the lowest band $J \cos \kappa$ analogous to the one-magnon case; as we consider $\omega \rightarrow 0$ in Figs.2 and 3, the driving phase is controllable. Wavepackets well-localized in momentum are standard in cold atom physics; provided the wavepacket is localized in position, directed transport as in Eq.(9), even the reversal of direction of travel with negative J , is possible. As experiment with a two species condensate, with different interactions, would mean that each species would access different resonances [5]. This would produce a more direct analogy with the behavior in Fig.3.

-
- [1] S. Bose, Phys. Rev. Lett. **91**, 207901 (2003); L. Amico, R. Fazio, A. Osterloh and V. Vedral, Rev. Mod. Phys. **80**, 517-576 (2008).
- [2] T.S. Cubitt and J.I. Cirac, Phys. Rev. Lett. **100**, 180406 (2008).
- [3] F. Grossmann, P. Jung, T. Dittrich and P. Hanggi, Z. Phys. B **84**, 315 (1991); M. Grifoni and P. Hanggi, Phys.Rep.**304**, 229 (1998).
- [4] A. Eckardt, C. Weiss and M. Holthaus, Phys. Rev. Lett. **95**, 260404 (2005)
- [5] C. Creffield and T.S. Monteiro, Phys. Rev. Lett.**96**, 210403 (2006).
- [6] H. Lignier, C. Sias, D. Ciampini, Y. Singh, A. Zenesini, O. Morsch, and E. Arimondo, Phys. Rev. Lett.**99**, 220403 (2007); A. Zenesini et al., Phys. Rev. Lett.**102**, 100403 (2009).
- [7] D.H. Dunlap and V.M. Kenkre, Phys. Rev. B **34**, 3625 (1986).
- [8] Q.Thommen, J-C Garreau, V Zehnle, Phys. Rev. A **65**, 053406 (2002); A. R. Kolovsky and H. J. Korsch, Int. J. Mod. Phys. B **18**, 1235 (2004).
- [9] S. Fishman, D.R. Grempel and R.E. Prange, Phys. Rev. Lett **49**, 509 (1982); F.L. Moore et al, Phys. Rev. Lett. **75**, 4598 (1995).
- [10] Y. Kayanuma and K. Saito, Phys. Rev. A., **77**, 010101(R) (2009).
- [11] L.F. Santos and M.I. Dykman, Phys. Rev. B **68**, 214410 (2003).
- [12] H. Bethe, Z. Phys. **71**, 205 (1931); Yu.N. Skryabin "Statistical Mechanics of Magnetically Ordered Systems", Kluwer Academic (1988). T.S. Monteiro, Phys. Rev. Lett. **96**, 187201 (2006).
- [13] T. Boness, K. Kudo, T.S. Monteiro, arXiv:0810.0454.